JOURNAL OF MATERIALS SCIENCE 27 (1992) 3883–3888

Growth characteristics of β-SiC by chemical vapour deposition

CHUN-HSUN CHU, YUNG-MING LU, MIN-HSIUNG HON
Department of Materials Engineering, National Cheng Kung University, Tainan, Taiwan

A twin-plane re-entrant corner effect (TPRE) in growth of chemical vapour deposited (CVD) β-SiC is described by the film and particles of gas-phase homogeneous nucleation. The structural morphology has been characterized by scanning electron microscopy and transmission electron microscopy. Morphological characteristics of the deposited crystals, such as triangularity, hexagons or facets have been explained in terms of the re-entrant corner effect at twin junctions, which were proposed as preferential growth sites for perfect crystals. For real deposits, screw dislocations and/or the re-entrant corner effect are not expected to be compatible. The majority of chemical vapour deposited SiC crystals have a high defect density comprised of {1 1 1} twins and dislocations associated with the process variables. Infrared transmission spectra and electron spectroscopy of chemical analysis indicated that the major chemical bonds of CVD β-SiC were Si–C and C–H bonds. The positions of the 1*s* or 2*p* core-level peaks for deposits are described.

1. Introduction

The film growth of a crystal from surface or dislocation nuclei, in an adsorption–desorption equilibrium of gaseous species, is generally understood in terms of the terrace–ledge–kink transport mechanism [1]. In the past, the growth of SiC has been shown to occur by two mechanisms: the deposition from solution on screw dislocations [2, 3] and the vapour–liquid–solid (VLS) mechanism for growing SiC whiskers [4, 5]. However, these mechanisms play a minor role in the growth of chemical vapour deposited (CVD) β-SiC deposits. The "re-entrant corner effect" was proposed to explain the growth of CVD β-SiC [6–8]. It should, however, be emphasized that the importance of the re-entrant corner was suggested originally for a perfect crystal surface, and that the influence of steps created by screw dislocations was not taken into consideration at that time. Later, the mechanism was also utilized to explain the growth of SiC in a CVD system. Kitamura *et al.* [9] focused their attention on re-investigating the validity of the re-entrant corner effect for twinned crystals which contained screw dislocations, and only flattened or elongated morphology of twinned crystals was discussed. In this study, we limited our concern to the contact twins in which a faceted, hexagonal or triangular morphology of CVD β-SiC was often observed. The features of β-SiC crystals grown by gas-phase homogeneous nucleation in the CVD process will be characterized and a twin-plane re-entrant edge mechanism for its growth proposed.

The kinetics of the deposition process and surface morphology of CVD SiC have been reported by many investigators [10, 11]. Recently, several investigations have utilized thermodynamic calculations to analyse the CVD of SiC from the Si–C–H–Cl gas system and thus to establish the requirement for single-phase growth of SiC [12, 13]. Because CVD involved a nucleation and growth process, research was mostly concentrated on the ideal thermodynamical aspects, whereas relatively few researchers were in a position to compare calculated results with experimental observations. Therefore, this work includes an analysis of the chemical constituents among the deposits and presents a detailed evaluation for a specific case in our deposition system to interpret certain aspects of the kinetics.

2. Experimental procedure

The growth of β-SiC deposits by thermal decomposition of methyltrichlorosilane (MTS, CH_3SiCl_3) in a hydrogen flow system was carried out in a cold-wall-type horizontal double-tube quartz reaction chamber in which the substrate, a clean graphite plate, was heated with a 450 kHz, 30 kW r.f. induction power supply. The substrate was precleaned and preheated above the deposition temperature in hydrogen for a minimum of 30 min prior to each deposition run. The substrate surface temperature was measured with an optical pyrometer. The concentration of CH_3SiCl_3 was controlled by flowing hydrogen through it at 0 °C at a fixed gas pressure. Hydrogen flow rates were measured from a calibrated flowmeter. The total gas pressure in the reaction chamber was maintained at 0.53 MPa.

The surface morphology and cross-sectional microstructure of the grown films and particles were observed by scanning electron microscopy. However, the SEM cross-sectional observations were made on

0022–2461 © *1992 Chapman & Hall*

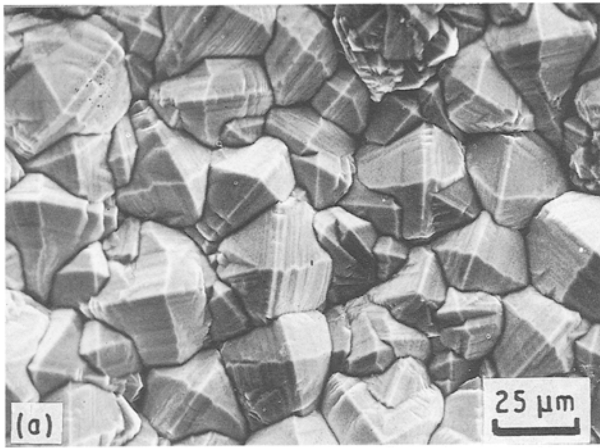

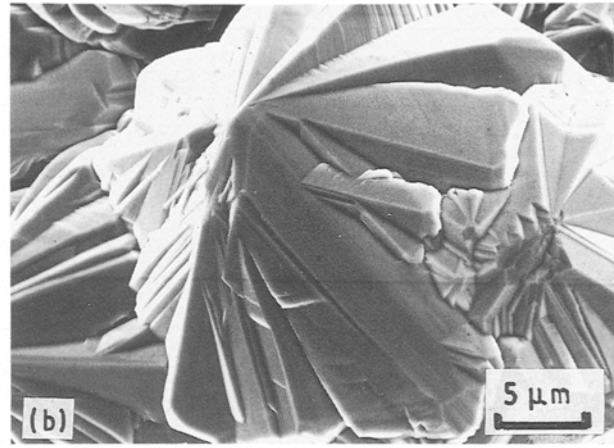

Figure 1 SEM surface morphology of a typical CVD β-SiC twin-faceted structure. (a) Four-fold symmetry faceted crystal. (b) Multi-star tip-faceted crystal, formed with an interpenetrant rotation twin.

samples etched at 110 °C for 5 min in an NaOH + $K_3Fe(CN)_6$ melt [14] in order to examine features of the lateral surface. The ion-beam milled samples were prepared for microstructural characterization by transmission electron microscopy. The crystal structure and orientation were analysed with an X-ray diffractometer at a wavelength of 0.15418 nm (CuK_α). The composition and chemical bonds in the films were examined by infrared transmission spectra (IR) and electron spectroscopy of chemical analysis (ESCA). The X-ray used was the MgK_α line at 1253.6 eV.

3. Results and discussion

3.1. Films and particles

A twin-plane re-entrant edge (TPRE) mechanism was proposed to account for the growth of CVD β-SiC [15]. In this mechanism, ease of propagation arose through the formation of re-entrant corners at the intersection of the twin planes, which made this location a favourable site for nucleation.

Fig. 1 showed a surface morphology of the β-SiC faceted structure on which the twin-plane re-entries were observed. In addition to the group of twin planes performing a typical four-fold symmetry faceted structure, cubic crystals of point group $\bar{4}3$ m, exhibiting the forms {1 1 1} and {1 1 $\bar{1}$}, were always observed, as shown in Fig. 1a. Interpenetrant rotation twin configurations extending in the radial direction of {1 1 1} faces and [1 1 1] twin axis (Fig. 1b) were observed. More than two components of the twinned crystal are joined only on an interface parallel to a lattice plane; in interpenetrant twins the interface between these twin components is often intimately intergrown, as shown in Fig. 1b.

Fig. 2 illustrates contact twinning in a cubic crystal of point group $\bar{4}3$ m which exhibited the two complementary forms {1 1 1} and {1 1 $\bar{1}$}. A contact twin in which twinning was formed by rotating about the normal to (1 1 1), which was, of course, parallel to the zone axis [1 1 1] in the cubic system. The angular relationship between the faces of twinned crystals is shown clearly in this figure. When a contact twin is joined in this manner, the ideal angle between the {1 1 1} planes bounding each other is 70.5°; therefore, the groove angles of these planes make angles of 141° and 219°. For the growth particles to select surface sites according to their energy preference, the phase should be sufficiently close to equilibrium so that they had enough time to find their appropriate sites (the 141° groove angle positions) during surface diffusion. When multiple twins with even components occurred, the contact twins would have three preferable sites on which to nucleate and propagate. The crystal growth with the re-entrant corner effect can therefore be expected to occur along three directions, perpendicular to the three groups of 141° groove lines, and have characteristics of triangular surface morphology and a (1 1 1) preferred orientation in the crystal. This is the same reason by which the multiple contact twins with odd components should have hexagonal microstructure and (1 1 1) texture.

From the above observations and discussion, the growth of β-SiC deposits might be described as follows. The growth of β-SiC can be attributed to ledge movement associated with twin planes. The crystal twinning could occur as a stacking fault during

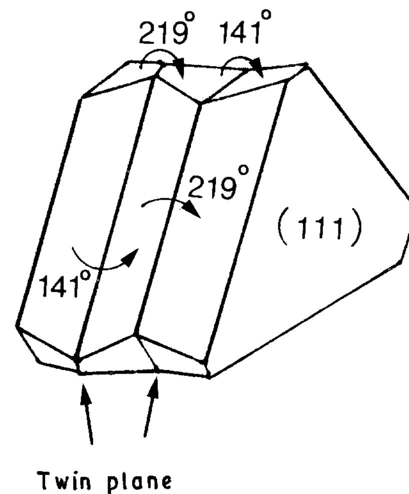

Figure 2 A schematic diagram of contact twinning in a cubic structure. All planes in this figure are always {1 1 1} faces and the groove angles are 141° and 219°.

crystal growth and/or when two nuclei coalesce and rotate into a precise twin relationship [15]. During crystal growth, atoms layers nucleated at the centreline of the grooves (141° groove positions) then spread upwards until they touch the ridge and come into contact with the new nuclei of neighbouring grooves to form continuous serrated growth layers. Consequently, the serrated steps which had a lower activation energy for incorporation of growth units, move along the re-entrant edges or growth facets and lead to the growth of film. However, unfortunately, we cannot find this crystal growth behaviour in our previous experiments on the growth of CVD β-SiC films.

From the discussion, it was considered that the TPRE mechanism develops in three dimensions, but crystal growth in the real deposits was only in two dimensions. Fig. 3 shows the cross-sectional morphology of the CVD β-SiC structure. It is clear that the grain size increases with increasing deposition time and each grain will become attached to the neighbouring grains during the deposition process. Only the absorption species on the grain surface could find their favourable locations for growth, and the growth direction of the thin film was perpendicular to the substrate. Other growth directions, parallel to the substrate, will be constricted by each other. With the competition of the films' growth, a typical fourfold symmetry faceted structure and multiple faceted structure were investigated in the CVD β-SiC films. No triangularity and/or hexagonal structures were observed, which are the growth characteristics occurring with the TPRE growth mechanism. Therefore, the assumption was made in our experiment, that if the deposit was grown by gas-phase homogeneous nucleation and propagation, the growth particles would not be affected by other particles in the gas phase, and a typical TPRE growth characteristic will be expected to reveal this crystal behaviour.

Fig. 4 shows the surface morphology of the β-SiC particles on which the triangular and hexagonal deposits grown by the TPRE mechanism using the gas-phase homogeneous nucleation method were observed. Under suitable experimental conditions, such as high deposition temperature and/or high total pressure, the homogeneous reaction is accelerated by the increase in intermolecular collision frequencies and the supersaturation of the reactants [16]. The vapour-phase homogeneous reactants form SiC particles and other by-product gases such as HCl; these then grow into drops at the substrate surface. The reactants in the vapour phase are depleted in a homogeneous reaction forming SiC particles, before the reactant gases are transported to the substrate surface. Therefore, chemical bonding between the grown particles

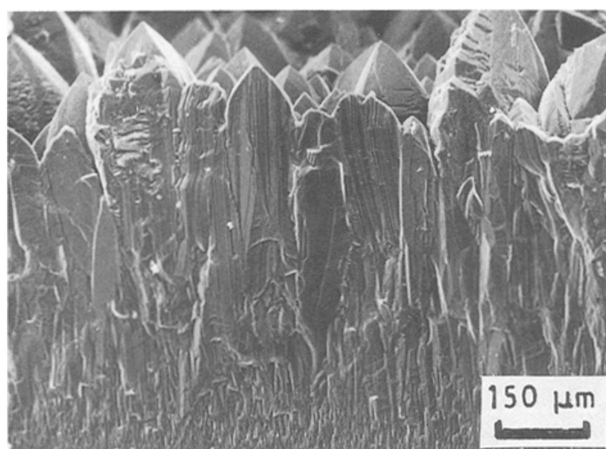

Figure 3 SEM lateral surface morphology of the CVD β-SiC faceted structure.

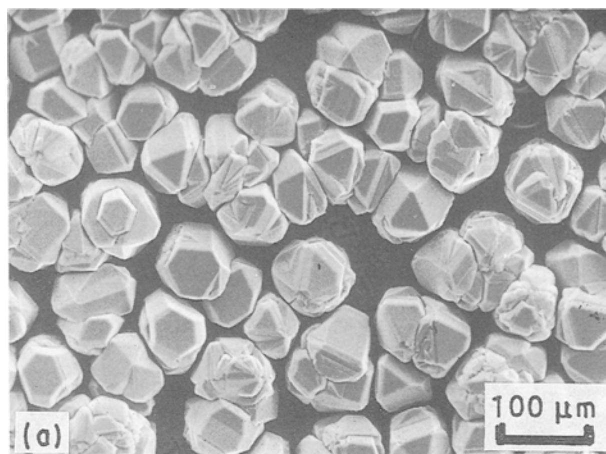

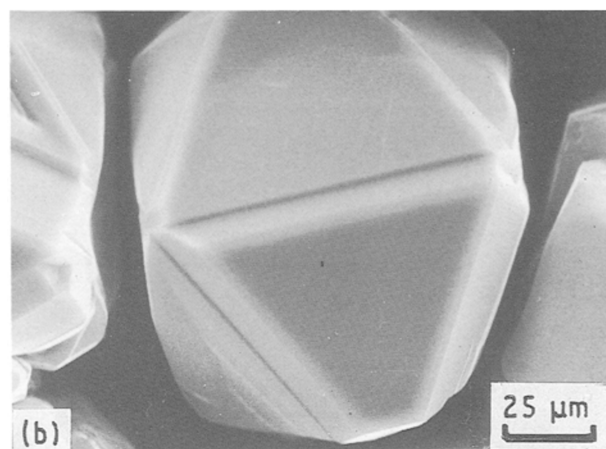

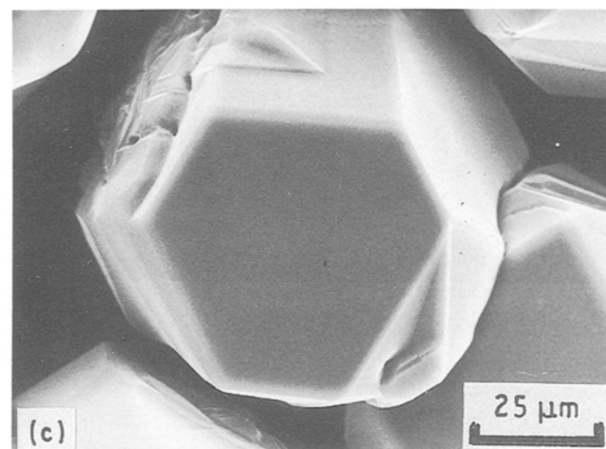

Figure 4 Scanning electron micrographs of the CVD β-SiC coating particles growing by the TPRE mechanism, using the gas-phase homogeneous nucleation method. (a) A typical facet, (b) triangularity, (c) hexagon.

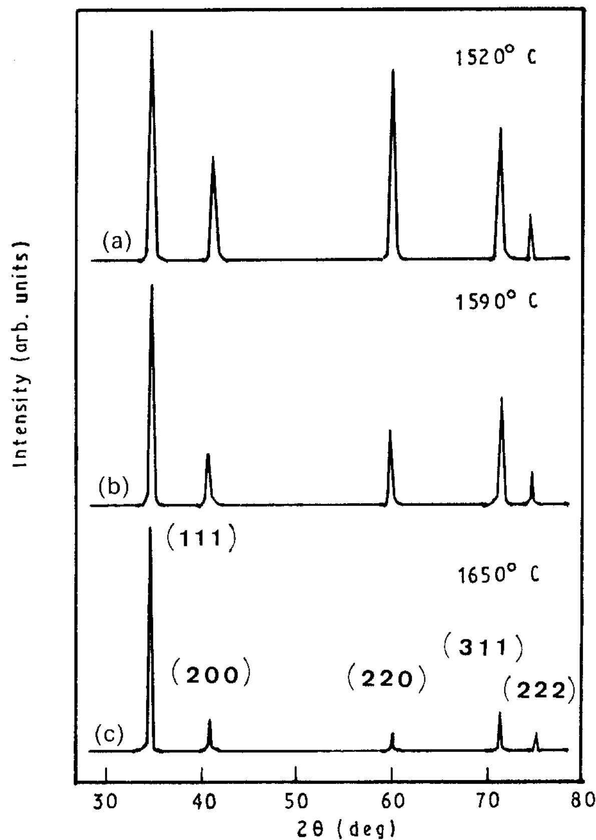

Figure 5 X-ray diffraction patterns of CVD β-SiC grown by gas-phase nucleation at (a) 1520 °C, (b) 1590 °C and (c) 1650 °C.

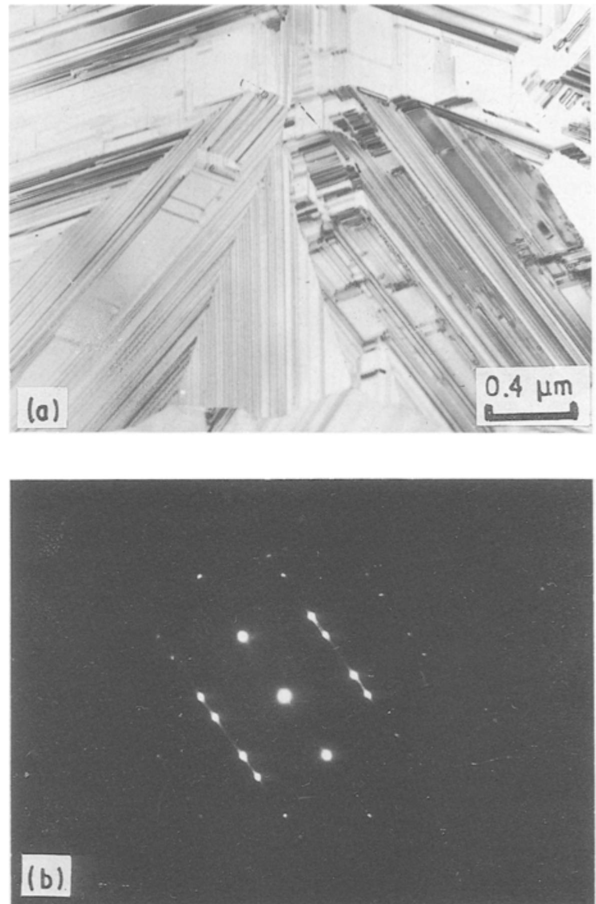

Figure 6 A typical transmission electron micrograph of CVD β-SiC deposit. (a) Bright-field micrograph of a (1 1 0) specimen. (b) Diffraction pattern showing the (1 1 0) pattern, as well as extra spots and streaks, indicating that the microtwin was present on (1 1 1) planes.

and substrate surface is very poor. These particles could be easily scraped away from the substrate, just by using a pencil. The X-ray intensity of the deposits obtained at different reaction temperatures is shown in Fig. 5, in which the major preferred orientation was (1 1 1) texture, not the (2 2 0) texture as detected in conventional thin films [11, 17], and the intensity of the (1 1 1) diffraction peak increased with increasing deposition temperature. The resulting deposit morphology and texture are explained in terms of the higher mobility of the absorption species, and thus they have sufficient time to find the most preferential sites at which to be incorporated into the crystal. From the above discussion, it is speculated that the TPRE mechanism should be the growth mechanism of CVD β-SiC.

3.2. Defects

Fig. 6 is a typical transmission electron micrograph of faceted β-SiC films. By examining the appearance of the growing crystals, a terrace–ledge–kink structure and narrow twins with different thicknesses were found (Fig. 6a). From the corresponding diffraction pattern (Fig. 6b), the planar defects were determined to be microtwins on the (1 1 1) planes. As shown in this figure, the planar defects of twins in the CVD β-SiC faceted structure are important, because their density is extremely high, and the line defects of dislocations are not easily examined.

Under high supersaturation, the adsorbed species could easily form two-dimensional nuclei on the surface before they found the most energetically favourable site, so that any site will have a similar preference for the adsorption of growth particles and two-dimensional nucleation will virtually take place everywhere on the surface. The re-entrant corner effect will not, therefore, be expected to operate at all under high supersaturation. Line defects of dislocations were examined on the CVD β-SiC films at high supersaturations, as shown in Fig. 7. The resultant characteristic morphology of CVD β-SiC crystals which have been

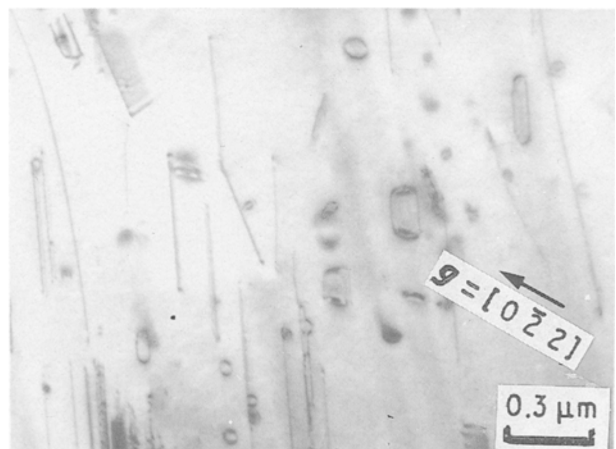

Figure 7 The bright-field image of a screw dislocation in CVD β-SiC under high supersaturation.

Figure 8 SEM surface morphology of CVD β-SiC dome-shaped structure with screw dislocations.

affected by screw dislocation propagation, revealed a dome-shaped structure instead of a faceted one, as shown in Fig. 8. Because the screw dislocation was a more preferable site than any other site on a perfect crystal surface, it was clear that preferential growth will take place at screw dislocations exposed at the twin junction. As screw dislocations existed in the CVD β-SiC films, the dislocation density increased with increasing reactive supersaturation and deposition time. As discussed above, the twin-plane corner effect, in its original sense, was only operative for a twinned crystal without screw dislocations when it grew under low supersaturation. When screw dislocations occur in a crystal, the growth mechanism will gradually change from TPRE to the screw dislocation growth mechanism by changing the supersaturation and deposition time.

3.3. Chemical constituents

As shown in Fig. 9, the infrared transmission spectra of β-SiC films showed that the deposit contained silicon bonded to carbon (as Si–C), and also hydrogen bonded to carbon (as C–H) etc. The analysis indicated that hydrogen was incorporated into the CVD β-SiC films, and/or films consisting of silicon, carbon and hydrogen. Fig. 10 shows ESCA detail scans of C 1*s* and Si 2*p* spectra of CVD β-SiC, and their standard binding energies. The results revealed that neither free silicon (99.15 eV) nor the carbon–oxygen single bond (290.2 eV), carbon–oxygen double bond (291.8 eV) and the carbon–chloride bond (292.2 eV) existed in the deposits. The standard binding energy of silicon in the Si–C bond was 103.9 eV and that of carbon in the Si–C bond was 285.7 eV, from the calibrated peak shift.

Thermodynamic calculations from chemical vapour deposition of the Si–C–H–Cl reaction system from several investigations [12, 13] were compared with our experimental results in order to analyse several features of kinetic mechanisms involved during deposition in the reactor. The kinetic mechanism of CVD β-SiC in the MTS–H_2 system might be described as follows:

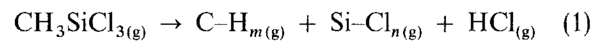

$$CH_3SiCl_{3(g)} \rightarrow C\text{–}H_{m(g)} + Si\text{–}Cl_{n(g)} + HCl_{(g)} \quad (1)$$

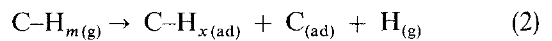

$$C\text{–}H_{m(g)} \rightarrow C\text{–}H_{x(ad)} + C_{(ad)} + H_{(g)} \quad (2)$$

$$Si\text{–}Cl_{n(g)} \rightarrow Si\text{–}Cl_{n(ad)} \quad (3)$$

$$H_{2(g)} \rightarrow 2H_{(ad)} \quad (4)$$

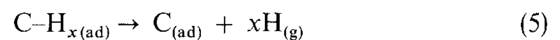

$$C\text{–}H_{x(ad)} \rightarrow C_{(ad)} + xH_{(g)} \quad (5)$$

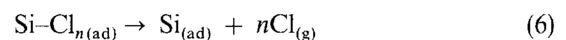

$$Si\text{–}Cl_{n(ad)} \rightarrow Si_{(ad)} + nCl_{(g)} \quad (6)$$

$$H_{(g)} + Cl_{(g)} \rightarrow HCl_{(g)} \quad (7)$$

$$Si_{(ad)} + C_{(ad)} \rightarrow SiC_{(s)} \quad (8)$$

(m, n, x = 0, 1, 2, 3). Equation 1 is described as the thermal decomposition step. The primary molecules carrying silicon are polar chlorides, whereas the primary molecules carrying carbon are simple non-polar hydrocarbons. The adsorption of gases on to the substrate surface is represented by Equations 2–4, and the chemical reactions of the adsorbed species, or of absorbed gaseous species are depicted as in Equations 5–7. In these equations, the chloride atom is completely desorbed from the surface to the bulk gas; the hydrogen atom in the adsorbed hydrocarbon is not entirely detached from the main flow gas. Finally, the

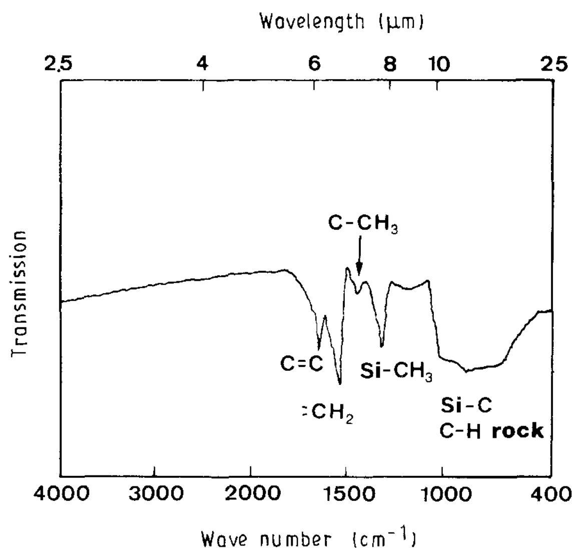

Figure 9 Infrared transmission spectra of CVD β-SiC.

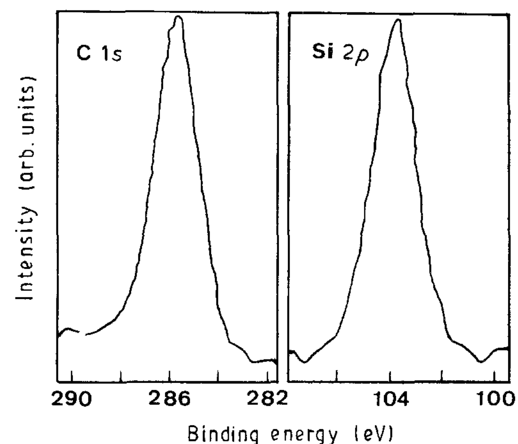

Figure 10 ESCA spectra of CVD β-SiC for the Si 2*p* and C 1*s* core-level peaks with MgK_α (1253.6 eV).

adsorbed species of silicon, carbon and trapped hydrogen diffusing to the most preferential sites are incorporated into the crystal by surface diffusion. The silicon carbide crystal would then grow by the formation of adsorbed species on the basal surfaces.

4. Conclusion

The propagation of CVD silicon carbide films was attributed to the twin-plane re-entrant edge mechanism. The TPRE growth mechanism operated under low supersaturation and for crystals without screw dislocations. For SiC crystals with screw dislocations under high supersaturation, the morphological characteristics of the TPRE growth mechanism are not clear. Numerous twins and dislocations were observed, associated with process parameters. ESCA and IR showed that the deposits contained silicon, carbon and hydrogen.

Acknowledgements

The authors wish to acknowledge the support of Chung Shan Institute of Science and Technology, and the National Science Council, which made this work possible.

References

1. N. GABRERA and R. V. COLEMAN, "The Art and Science of Growing Crystals", 3rd edn, edited by J. J. Gilman (Wiley, New York, 1963) p. 1.
2. W. F. KNIPPENBERG and G. VERSPUI, *Philips Res. Rep.* **21** (1963) 113.
3. G. W. SEARS, *Acta Metall.* **1** (1953) 457.
4. R. S. WANGER and W. C. ELLIS, *Appl. Phys. Lett.* **4** (1964) 89.
5. J. V. MILEWSKI, F. D. GAC, J. J. PETROVIC and S. R. SKAGGS, *J. Mater. Sci.* **20** (1985) 1160.
6. L. N. STRANSKI, *Disc. Faraday Soc.* **5** (1949) 66.
7. R. S. WANGER, *Acta Metall.* **8** (1960) 57.
8. W. F. KNIPPENBERG and G. VERSPUI, in "Silicon Carbide 1973", edited by R. C. Marshall, J. W. Faust Jr and C. E. Ryan, (University of South Carolina Press, Columbia, SC, 1974) p. 92.
9. M. KITAMURA, S. HOSOYA and I. SUNABARA, *J. Crystal Growth* **47** (1979) 93.
10. S. NISHINO, Y. HAZUKI, H. MATSUNAMI and T. TANAKA, *J. Electrochem. Soc.* **127** (1980) 2674.
11. J. CHIN, P. K. GANTZEL and R. G. HUDSON, *Thin Solid Films* **40** (1977) 57.
12. A. I. KINGON, L. I. LUTZ, P. LIAW and R. F. DAVIS, *J. Amer. Ceram. Soc.* **66** (1983) 558.
13. G. S. FISCHMAN and W. T. PETUSKEY, *ibid.* **68** (1985) 185.
14. J. M. HARRIS, H. C. GATOS and A. F. WITT, *J. Electrochem. Soc.* **116** (1969) 672.
15. D. J. CHENG, W. J. SHYY, D. H. KUO and M. H. HON, *ibid.* **134** (1987) 3145.
16. C. S. PARK, J. G. KIM and J. S. CHUN, *J. Vac. Sci. Technol.* **A1**(4) (1983) 1820.
17. M. G. SO and J. S. CHUN, *ibid.* **A6** (1985) 5.

Received 25 March
and accepted 1 July 1991